

Design and Implementation of a Microgrid-Capable Solar Inverter

by

Gavin M. Darcey

S.B., EECS, Massachusetts Institute of Technology (2011)

Submitted to the Department of Electrical Engineering and Computer
Science

in partial fulfillment of the requirements for the degree of

Master of Engineering in Electrical Engineering
and Computer Science

at the

MASSACHUSETTS INSTITUTE OF TECHNOLOGY

September 2013

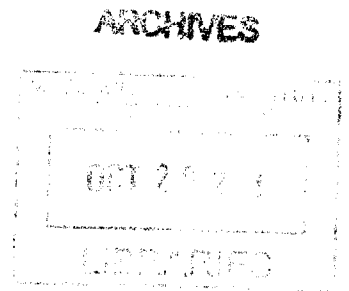
©2013 Gavin M. Darcey All rights reserved.

The author hereby grants to M.I.T. permission to reproduce and
distribute publicly paper and electronic copies of this thesis document
in whole and in part in any medium now known or hereafter created.

Author
Department of Electrical Engineering and Computer Science
August 30, 2013

Certified by
James L. Kirtley, Jr.
Professor of Electrical Engineering
Thesis Supervisor

Accepted by
Prof. Albert R. Meyer
Chairman, Master of Engineering Thesis Committee



Design and Implementation of a Microgrid-Capable Solar Inverter

by

Gavin M. Darcey

Submitted to the Department of Electrical Engineering and Computer Science
on August 30, 2013, in partial fulfillment of the
requirements for the degree of
Master of Engineering in Electrical Engineering
and Computer Science

Abstract

The notion of a practical microgrid - a small, interconnected system of generators and loads that operates both synchronously with a larger, centralized grid and isolated from the grid, autonomously - has grown popular as electric utilities are installed more frequently in areas lacking a pre-existing central grid. To research the effects of both intentional disconnects and unintentional faults within a microgrid and between it and the central utility, we have constructed such a system in simulation by using hardware to simulate the real-world generators and loads of the microgrid and have connected it to the MIT utility.[1] The microgrid requires a clean, efficient switching system in order to connect and disconnect its components, and this thesis begins with an explanation of the control hardware and software interface implemented to do so. Next, this thesis details the design of one of the main generating sources for the microgrid, the inverter for a hardware-simulated solar panel. Solar panels with DC output are virtually always connected through a power inverter to produce the usable three-phase AC on the power grid. This particular inverter design is intended to be control-scheme agnostic; the actual operation of it will vary with different control algorithms. It is designed to be a general purpose, three phase 2.3 kW power inverter, albeit with specifically added modules to suit this particular microgrid. This thesis covers both the design of the circuit and the finished layout of its printed circuit board.

Thesis Supervisor: James L. Kirtley, Jr.
Title: Professor of Electrical Engineering

Acknowledgments

I would like to thank Professor Kirtley for first giving me the opportunity to work on this project; his immense support bringing me on to the project and guidance throughout has been invaluable. I would also like to thank Jorge Elizondo Martinez, who was always ready to help answer any questions involving the inverter design, and finally Jared Monnin, Michael Zieve, and Zhiyong Wang for their enormous help during the beginning construction of the physical microgrid.

Contents

1	Microgrid Overview	8
1.1	Microgrid Layout	8
1.1.1	Loads	9
1.1.2	Interconnection	10
1.2	Control Interface	11
1.2.1	Control Software	12
1.2.2	Control Hardware	13
2	Inverter Design	15
2.1	High-power Stage	16
2.1.1	Three-phase Bridge	16
2.1.2	Output Filter	18
2.2	Gate Driver	19
2.2.1	IR21362S	19
2.3	Control Power and Signal Isolation	20
2.3.1	Optocouplers	20
2.3.2	Digital Isolators	21
2.3.3	Grounding	22
2.4	Signal Measurement	23
2.4.1	Voltage	23
2.4.2	Current	24
2.5	Signal Processing	25

3	Final Layout	27
3.1	Physical Footprint	27
3.2	Conclusion	30

List of Figures

1-1	Microgrid block diagram.	9
1-2	Microgrid loads.	10
1-3	Three-phase relay schematic.	11
1-4	LabVIEW backend code.	12
1-5	Switching control user interface.	13
1-6	Interface hardware.	13
1-7	SSR amplifier circuit.	14
2-1	Three-phase bridge topology.	17
2-2	Output filters.	18
2-3	Typical application of gate driver.	20
2-4	Optocoupler circuit.	21
2-5	Digital isolator circuit.	22
2-6	Voltage sensor circuit.	24
2-7	Current sensor circuit.	24
2-8	Signal processing circuit.	26
3-1	Overall view of circuit footprint.	27
3-2	Ground planes.	29

List of Tables

2.1 List of grounds used and circuit modules relative to them. 23

Chapter 1

Microgrid Overview

This chapter covers the overall microgrid construction, beginning with its physical layout in the LEES lab space, and finishing with the interconnection and switching system implemented as part of this thesis.

1.1 Microgrid Layout

The microgrid used in this project is a set of three hardware-simulated generators and six basic loads, intended to model a typical commercial load that would be connected to the grid. The current functioning generators are a linked electric motor set that represents a diesel-powered synchronous generator and a DC power supply linked to a power inverter, the design of which is detailed later in this thesis. The grid includes capabilities to add a third generator in the future, which will model a wind turbine generator system. Figure 1-1 on the next page provides an overall general schematic of the microgrid layout. The six loads are described in the next section.

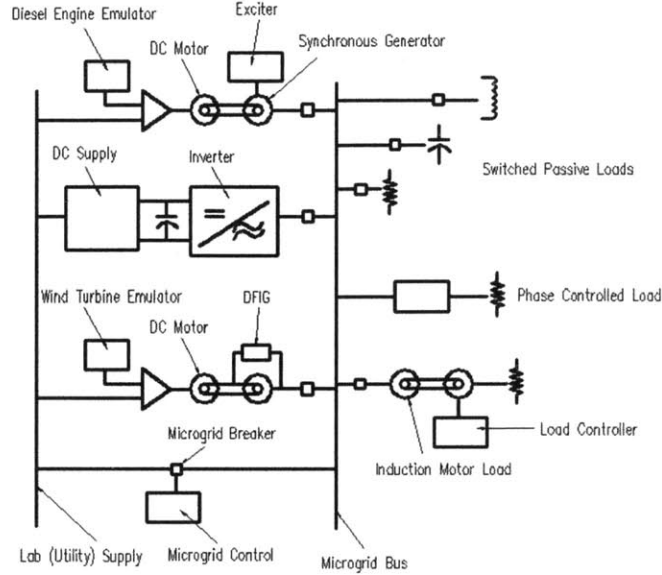


Figure 1-1: System-level block diagram of complete microgrid. Note that all inter-connection lines are three-phase AC. [3]

1.1.1 Loads

The loads themselves are all balanced, three phase sets representing different types of typical system loads. Included are two purely resistive loads, each made of three power resistors in a wye formation, tuned to 70Ω . There is a purely capacitive load constructed from six large AC $80\mu\text{F}$ capacitors and a purely inductive load made from three laminated iron cores with two air gaps and about 270 windings, for an inductance of about 108mH on each phase. These loads are also in a wye formation, and provide a total capacitive load of about 650VAR and an inductive load of 1.05kVAR , respectively.

Beyond these four basic RLC loads, the grid also contains two more complex loads, to model more realistic applications. The first consists of a phase-controlled load built from three single-phase light dimmers, mounted back-to-back with the levers mechanically coupled to control all phases simultaneously. Each dimmer is connected in series with a 60W incandescent light bulb, and the three dimmer/bulb pairs are again connected in a wye formation with the neutral point tied to the microgrid neutral line.

These dimmers, along with the first four loads, are shown in Figure 1-2 as they stand mounted on the microgrid.

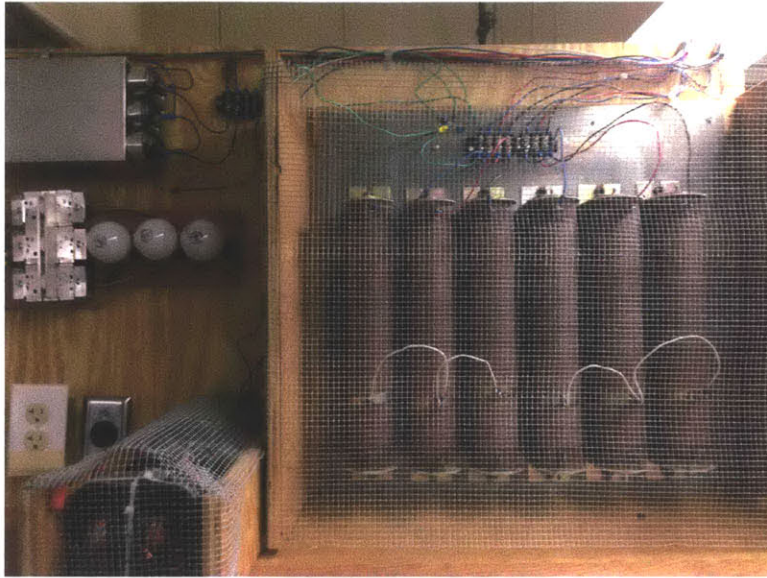


Figure 1-2: Photograph of loads physically mounted on microgrid. Clockwise from bottom left: inductors, phase-controlled light bulbs, capacitors, two resistor banks. Induction motor not pictured.

The final load is a 1HP squirrel cage induction motor mechanically tied to a 1.5HP DC motor. The induction motor is tied to the microgrid bus, while its linked DC motor exists to adjust the torque loading on the induction motor.

1.1.2 Interconnection

The connections between the loads and generators, as well as the complete microgrid and the MIT electric utility, are all handled through solid-state relays, specifically the Carlo Gavazzi RZ3A60A55. The relays link between each isolated microgrid subsystem and a central screw-terminal wire bus. These particular relays were chosen not only for their suitably high operational voltage tolerance and inherent three-phase connection layout, but also for their quick switching response time. Originally, only the generators and main grid connection were routed through solid-state relays; all load connections were handled through electromechanical relays which use solenoids to initiate contact. However, it was determined through testing that these electrome-

chanical relays included a switching delay when switched after being in a prolonged state of either on or off. For the sake of rapid disconnection at any time if necessary, all relays were switched to the solid-state models. Figure 1-3 shows a schematic of the solid-state relays that link each component to the main bus.

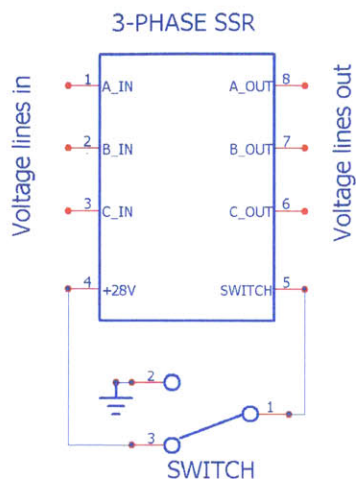


Figure 1-3: When the switch is moved to position 2, a +28V potential difference will sit across the control pins and all three phases will conduct. This switch models the control hardware discussed in Section 1.2.2.

1.2 Control Interface

The control of these relays has been implemented using the National Instruments LabVIEW design platform. It was determined early in the project that the project would need signal monitoring and measurement capability added to several places throughout the microgrid, which was to be done using several National Instruments data acquisition devices (DAQs). This has since been successfully built but remains outside the scope of this document. However, the software and hardware that comprise the control system, which also relies on the DAQs, are detailed in this section.

1.2.1 Control Software

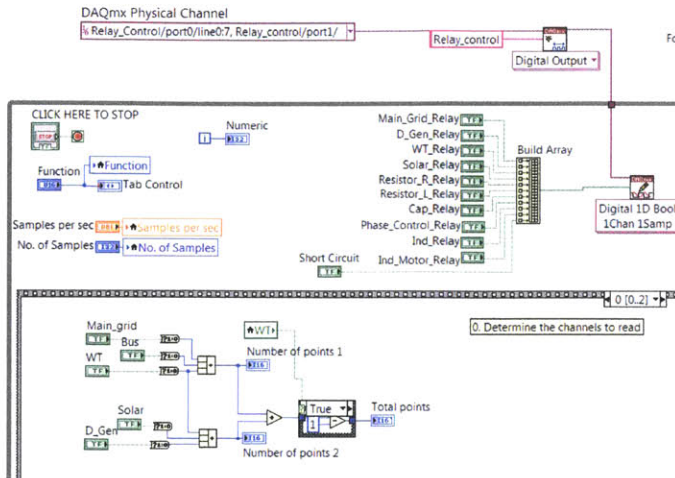


Figure 1-4: Code snippet from LabVIEW backend control code, used for connecting and disconnecting relays.

LabVIEW is essentially a graphical programming language, which allows the programmer to write code using flow diagrams that are then continuously executed when run. When running, the user is presented with a front-end control panel that allows for interaction with the code running in the background. The front control panel for the microgrid, when executed, waits for the user to click on-screen pushbuttons, the state of which is stored in a binary array. This array is 11 characters long, with one bit reserved for each of the three generators, six loads, and one MIT utility connection. The eleventh bit is used to initiate a short circuit by way of controlling a separate solid-state relay which shorts the three phases of the utility line. It is intended to model an accidental fault across the microgrid for future islanding (main utility disconnection) experiments. As each button is pressed, an on-screen LED will light up to indicate the relay is currently conducting, matching the the physical relay indicator as well. Figure 1-4 is a screen capture of the main component of the backend LabVIEW code and illustrates the sequence that is run by the control panel, while Figure 1-5 on the following page presents the user interface for switch control. The current microgrid interface includes significantly more capabilities beyond the basic switch control, such as data measurement and plotting, but that work was done outside of this thesis.

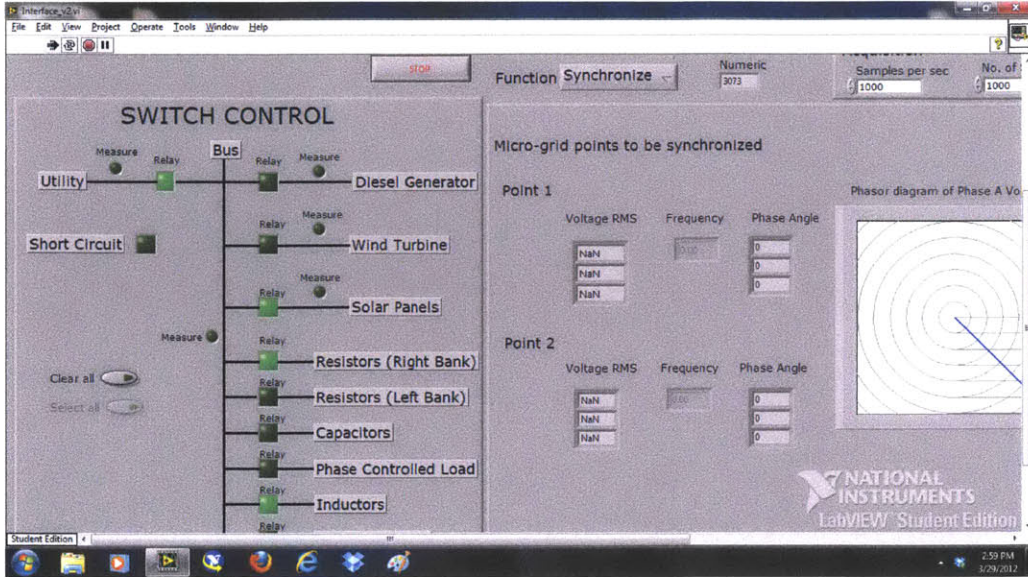


Figure 1-5: User-facing control panel when LabVIEW code is run. When the green buttons are pressed, the relays are activated and the on-screen LED lights up.

In addition to the separate pushbuttons for each relay, additional controls have been created to initiate all connections or disconnections simultaneously. This was implemented both for convenience when testing the grid and for safety; in the event of an actual, unintended fault all loads and generators can be disconnected quickly right from the control panel. These can be seen in Figure 5 as well.

1.2.2 Control Hardware

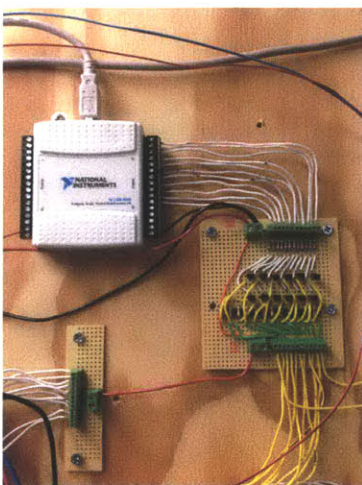


Figure 1-6: Left: DAQ for relay control. Right: array of BJT amplifier circuits to read DAQ input and switch relays.

Figure 1-6 on the previous page shows the two pieces of relay control hardware. The LabVIEW code runs on a National Instruments USB-6008, a low-cost USB-powered multifunction DAQ with 12 digital input/output (I/O) pins. Eleven of these pins are tied to the software's eleven-bit binary array, and appropriately output a transistor-transistor logic (TTL) level of 0V or +5V as on-screen buttons are pressed. Each I/O pin output is then sent to its own common-emitter amplifier (CE) circuit, a schematic of which is seen below in Figure 1-7:

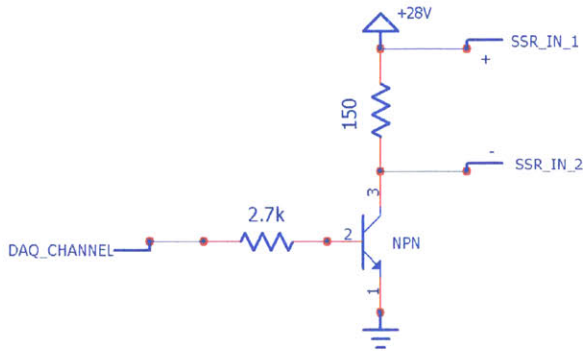


Figure 1-7: Schematic for pull-up CE amplifier to quickly switch solid-state relays according to DAQ output.

This pull-up circuit is necessary because the relays require a minimum of +24VDC at their connection terminal, which is above the capable TTL output range of the DAQ. Additionally, the relays must be turned on quickly, which requires more current than can be sourced by the DAQ alone. The arrangement of common-emitter amplifiers, with their power rails tied to an external wall power supply tuned to +28V, is able to activate and deactivate the relays with appropriate speed. It should be noted that in order to control the amplifier circuit reliably, the ground pin of the DAQ must also be tied to the ground line of the external +28V power supply.

Chapter 2

Inverter Design

A common power source in existing microgrids is a photovoltaic (PV) array, which must have its DC output sent through a power inverter in order to generate the appropriate AC waveforms to handle commercial appliances. For this microgrid, commercially available inverters were purchased - three Enphase D380 microinverters. These three single-phase inverters were tied together and connected to the grid just as intended. However, it was soon discovered that these were inadequate for this specific project due to standard industry regulations.

Underwriter Laboratories (UL) 1741 - *Inverters, Converters, Controllers and Interconnection System Equipment for Use With Distributed Energy Resources* - and IEEE 1547 - *Standard for Interconnecting Distributed Resources with Electric Power Systems* both dictate the acceptable behavior of a solar inverter while in use [6] , and as per IEEE Std 1547.2-2008 8.1.5: “The DR [distributed resource] shall not energize the Area EPS [electric power system] when the Area EPS is de-energized.” [2] This requirement is intended to ensure the safety of any utility personnel working in a nominally deactivated area; all distributed resources such as solar panels are required to shut off completely if the rest of the grid is disconnected. In other words, with no detected outside grid voltage, commercial inverters cannot source their own voltage.

While perfectly reasonable for a commercial product designed for constant utility connection, this requirement renders the Enphase inverters unusable for the microgrid islanding experiments. It was deemed necessary to design a custom three-phase inverter capable of sustaining voltage output regardless of grid connection. This chapter details the microgrid inverter design completed as part of this thesis.

2.1 High-power Stage

The main function of the inverter is to convert a large DC voltage - modeling a photovoltaic array - into the standard three-phase AC distribution of three separate 60Hz sine waves, each 120 degrees out of phase. This requires both rapid switching of three sets of transistor pairs and filtering on the output to eliminate unwanted harmonics.

2.1.1 Three-phase Bridge

The inverter relies on the canonical three-phase bridge topology common to most three-phase inverters. It consists of three sets of high/low pairs of MOSFETs (with each pair commonly called a “totem”), where the top MOSFET of each totem is tied to the high level of the modeled PV array. The inverter has been designed to operate with a DC input of as high as +230V. The low MOSFET is then tied to the ground of this high voltage, referred to in this design as COM. The three-phase bridge is shown in Figure 2-1 on the next page.

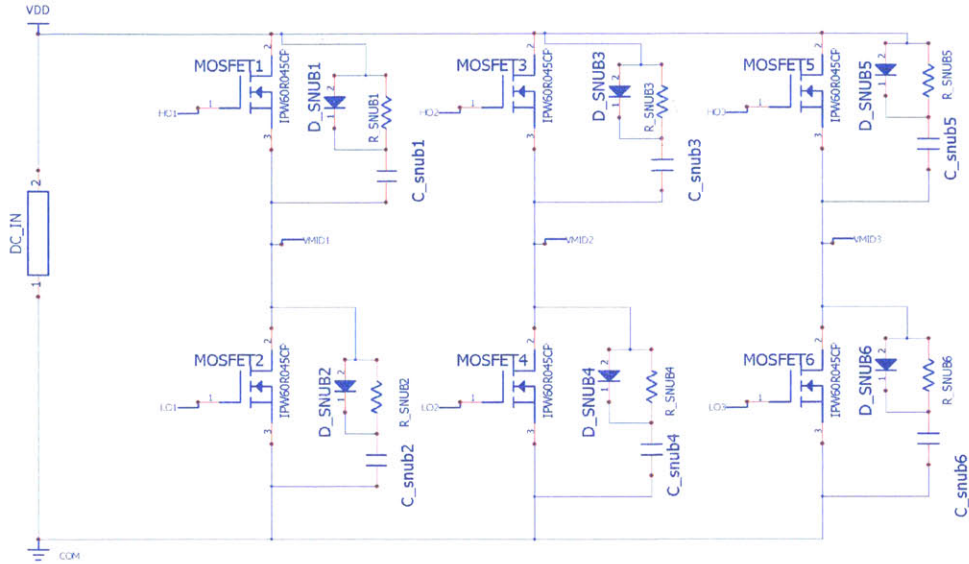


Figure 2-1: Common three-phase bridge topology consisting of three pairs of high and low MOSFETs, each with their midpoints being sent out to filter.

Each MOSFET also includes a snubber circuit designed to limit stresses on the semiconductor switches. Although the MOSFETs are all rated to withstand a +600V potential across their drain and source, the stresses while switching coming from parasitic inductances may place unanticipated strain on them. The snubber circuit is a practical turn-off snubber [4] consisting of a single diode in parallel with a resistor, the combination of which is in series with a capacitor. The capacitor presents a third path for current to flow when the MOSFET is turned off, while the resistor is included to limit the capacitor's discharge current when the switch is turned back on. Although optimized efficiency was not the goal of the inverter, the diode is provided to allow the capacitor charging current to avoid the resistor when the switch is turned off.

2.1.2 Output Filter

The output of each phase from the three-phase bridge is sent through a filter before being delivered as the final output. The filter designed for this inverter consists of two inductors and a capacitor on each phase, as seen in Figure 8.

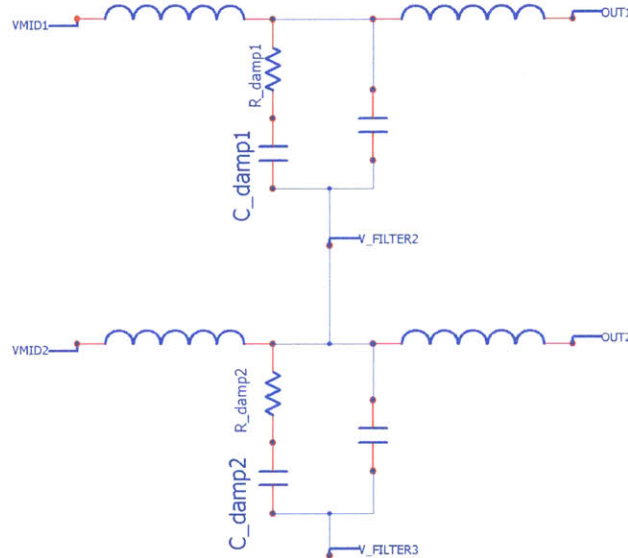


Figure 2-2: Schematic illustrating two of the three output filters, where VMID1 and VMID2 come directly from the totem midpoints in Figure 2-1. Also note that the filters all connect line-to-line.

The filter components are currently not yet sized; the physical board layout allows for a general iron core to be fitted with as many windings as necessary for the inductors, and an extremely common capacitor footprint is used to allow for a wide range of capacitor values to be used. This is due to the fact that a control scheme has not yet been finalized; the filter specifications will depend on the switching algorithm used on the MOSFETs.

Also included is a damper circuit to avoid resonance peaks while operating. This damper circuit is a simple series RC that sits in parallel with the main filter capacitor. Finally, it should be explicitly noted that the three phases of the inverter output are all defined as line to line, rather than line to neutral or line to ground.

2.2 Gate Driver

The MOSFETs in the totem bridge are intended to be controlled through either a microcontroller or digital signal processor (DSP), but these devices are not capable of sourcing and sinking the current necessary to quickly charge and discharge the MOSFET gates. Hence, a gate driver circuit must be used to effectively and rapidly switch the MOSFETs.

2.2.1 IR21362S

To drive the MOSFET gates, it was deemed practical to use a monolithic three-phase gate driver IC, which provides a single chip to interface with all six MOSFETs and requires minimal outside circuitry. This inverter uses an International Rectifier IR21362S chip, which includes built-in shoot-through delay to ensure that any particular high/low pair never has both its switches on. Doing so would short the high input voltage (VDD) to COM, potentially causing damage both to the modeled PV array and the inverter. Of the IR2136 family of ICs, the IR21362S was chosen due to its active-low low side inputs. This allows for the normal 6-input control scheme, as well as 3 inputs fed directly to the driver with the driver's high/low inputs shorted together for each respective phase. The shoot-through delay ensures that either control scheme will function properly. For testing purposes, the driver chip was wired up on a prototyping board as according to Figure 2-3 on the next page, the typical connection scheme from its data sheet.[5] The phase inputs were paired together in the 3-input control scheme with a 10kHz square wave given as input. This confirmed the suitability of the driver chip for this application and the presence of a sufficient shoot-through delay, measured to be about 240ns. The complete driver schematic as it sits on the inverter board uses this same arrangement.

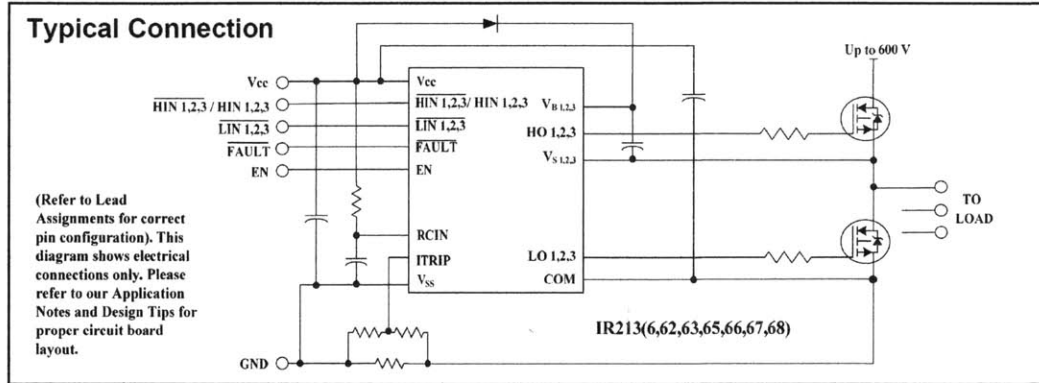


Figure 2-3: Typical application arrangement of gate driver IC, as given by manufacturer. [5]

2.3 Control Power and Signal Isolation

The inverter is powered by a DC wall supply, designed to nominally be set at +30V. However, this input requirement is not strict as the board uses a CUI VYB15W DC/DC converter to maintain 2 power rails around the board for control power purposes. The converter outputs both +15V and -15V, relative to its own 0V output and will maintain these outputs so long as the DC input is between +18V and +75V. The 0V is distributed around the board as an analog ground for the control circuitry and presents a level of galvanic isolation between the DC wall supply and the component power rails. Along with the $\pm 15V$ supply traces, there are several 7805 linear regulators around the inverter to power both sensing circuits and isolators.

Because of the high-power capabilities of the inverter, it is necessary to electrically isolate all control signals from the power stage to avoid damaging the control hardware. This is first accomplished at the input to the gate driver, which can be isolated from its source (either the microcontroller or DSP) in one of two ways, either through optocouplers or digital isolators.

2.3.1 Optocouplers

Prior to arriving at the driver IC, the six gate signals each route through a Vishay MOC8101 optocoupler, with its output phototransistor in a common-collector amplifier circuit arrangement. In addition to the $1k\Omega$ pull-down resistor, the optocou-

pler circuit also includes a current-limiting resistor at the input to the optocoupler, which prevents the control hardware from over-sourcing current. Figure 2-4 shows a schematic of the complete optocoupler circuit that isolates each gate driver input. It should be noted that the +5V power rail for the optocoupler comes from a dedicated 7805 IC mounted near the optocoupler area of the inverter, and each optocoupler chip is also provided a .1 μ F bypass capacitor near its power pin.

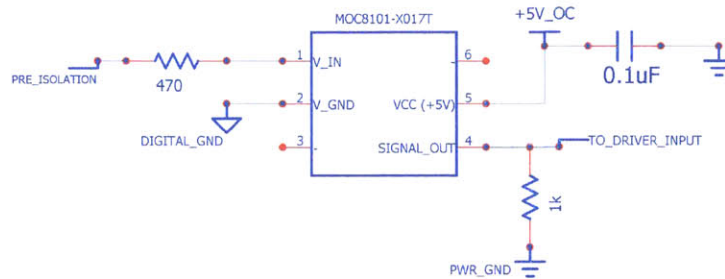


Figure 2-4: Complete schematic of optocoupler isolation for one driver input. Signal on left comes directly from microcontroller or DSP, while signal on right is routed directly to gate driver.

2.3.2 Digital Isolators

Because the optocouplers require some external circuitry and are relatively slow in their signal transitions when in use, a set of Avago HCPL-9030 digital isolators has also been included on the inverter. While the outputs of both the digital isolators and optocouplers are tied together at the gate driver inputs, only one must be used while operating the inverter. It is assumed that the digital isolators will be primarily used, given their faster output rise/fall times. The optocouplers have a rise and fall time of 2 μ s, while the digital isolators are between 2 and 4ns. The optocouplers will be adequate for operating the inverter, but the isolators provide a tighter level of control should a higher switching frequency be desired.

The digital isolators are much simpler to use as well, as seen by their complete circuit schematic in Figure 2-5. The optocouplers remain a part of the inverter topology as a failsafe, so that control signals may still be isolated and sent to the gate driver in the event that one of the digital isolators fails.

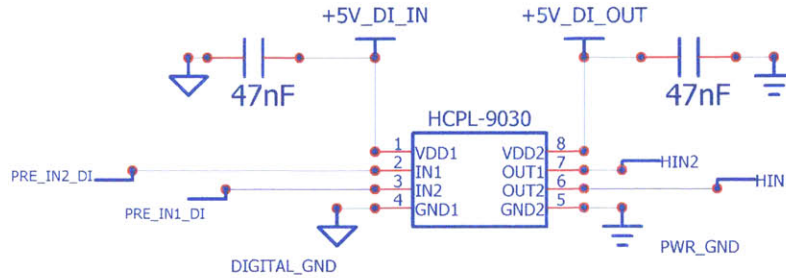


Figure 2-5: Each digital isolator chip is capable of isolating two independent signals, and has an overall less complex footprint.

2.3.3 Grounding

Because of the various isolated sections necessary for the board to operate with sufficient protection for the control and measurement hardware, there are five separate ‘grounds’ used on the inverter, all completely separated from each other on the physical board. First, the inverter analog ground provided by the DC/DC converter’s 0V output is isolated from the DC wall supply (‘wall ground’) as previously mentioned. However, as the gate driver operates on the three-phase bridge between the high voltage PV array and its own common level, COM, the power supply for the gate driver must be relative to a separate power ground, with both this power ground and COM connected to the driver chip through a trio of sensing resistors. This can be seen back in Figure 2-3, the typical IR21362S connection. This extra isolation between the main inverter power supply and the gate driver power is done through another DC/DC converter, a TI DCP010515. Finally, the digital drive signals from the microcontroller/DSP are also isolated through either the optocoupler or digital isolator circuit as mentioned in the previous section. These drive signals are relative to another, unique, digital ground. Note that the digital and analog grounds should be connected together via a single wire when using the inverter. They are explicitly

separated on the circuit design but connect at a single intersection to reduce unwanted noise, as is common in circuit design. Table 2.1 presents a concise view of the various grounds and the modules that relate to them.

Wall ground	wall-plugged DC source used for board power
COM	wall-plugged high voltage DC source modeling PV array
Power ground	driver IC, optocoupler/isolator output
Analog ground	voltage/current sensors, signal processing units
Digital ground	optocoupler/isolator input, microcontroller/DSP

Table 2.1: List of grounds used and circuit modules relative to them.

2.4 Signal Measurement

As the inverter is designed to operate as a module within the microgrid, it is necessary to include measurement hardware to monitor various voltage and current levels on the board; these measurement signals are read by monitoring boards throughout the microgrid and sent to the main LabVIEW interface for control purposes. While there are several spots on the inverter for measurements to be made, this section discusses the design of the voltage sensor and current sensor circuits. The discussion of the locations of the the actual sensors is presented in Chapter 3.

2.4.1 Voltage

The voltage sensor used in the inverter is the LEM LV 20-P, which draws a minimal amount of current (10 mA) while remaining capable of measuring up to a 500V difference between its input terminals. It does require two external resistors - one resistor between the high voltage to be measured and high input pin, and one resistor at the measurement output pin. The high voltage resistor presents some difficulty - ideally, it should be a precision resistor with a tolerance of $\pm 1\%$ in order to provide accurate measurements. Sufficiently high power-rated precision resistors that can dissipate the necessary heat are not common, but the Riedon PF1262-20K 20k Ω precision resistor is capable of dissipating up to 20W with an adequate heat sink

affixed to it. Figure 2-6 shows the general schematic for each of the voltage sensors placed on the inverter board.

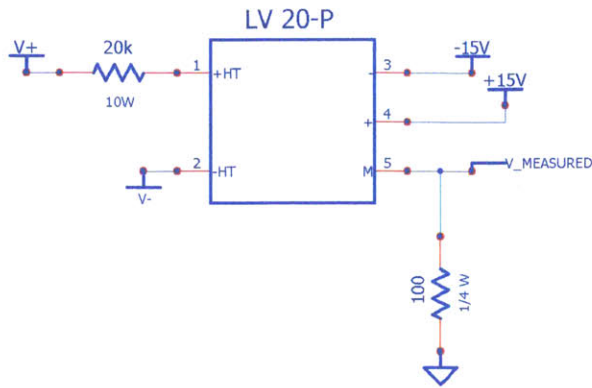


Figure 2-6: Circuit used for voltage sensing throughout the inverter board. V- does not necessarily need to be grounded.

2.4.2 Current

The Allegro ACS712 current sensors used in the inverter board require some very minor supplementary components to operate as well. An external capacitor is used to set the device bandwidth; for the microgrid measurements a capacitance of 1nF is adequate, as seen in Figure 2-7. The primary difficulty with the current sensor is its need to be physically close to the copper traces being measured, which proved challenging given the wide power traces necessary on the inverter.

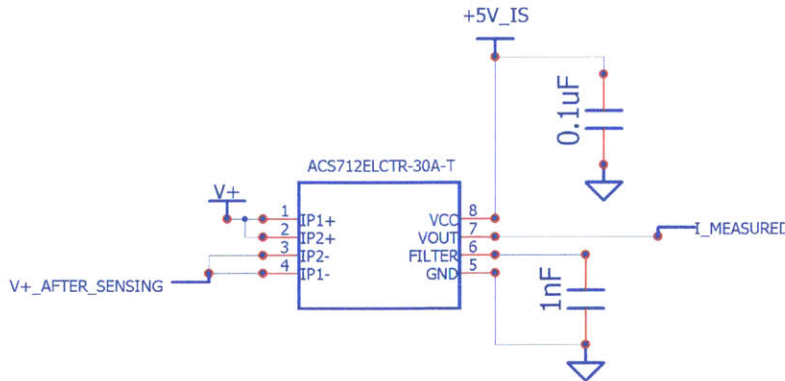


Figure 2-7: Circuit used for current sensing throughout the inverter board. The traces must be routed directly through the sensor IC.

2.5 Signal Processing

The final circuitry designed for the inverter is related more to interfacing with the microgrid system than the inverter itself. The digital measurements being output by the various sensors are between $\pm 2.5V$, but must be shifted to levels between $0V$ and $+5V$ in order to be processed by the external microgrid monitoring hardware. Note that these signals are still analog as they are precise measurements, not digital control logic. To accomplish this, six separate signal processing units have been included in the inverter design, with their inputs and outputs made easily accessible via screw terminal blocks for any external signal to be processed. Each unit is a TL071 op-amp in a summing amplifier configuration, with a $-5V$ reference level at one input and the measurement signal to be shifted at the other. The summing amplifier follows equation 2.1

$$V_{out} = \frac{R_{feedback}}{R_{in}} \times (V_{in} - 5V) \quad (2.1)$$

For example, an input signal of $-2.5V$ would be altered to $+3.75V$ for further processing by the microgrid. An LC output filter and damper is also included, although these are all very small surface mount components, unlike the filter and damper designed for the power stage. The $-5V$ reference level is set using an AD588 voltage reference. Figure 2-8 on the following page presents both the voltage reference circuit and an example signal processing unit.

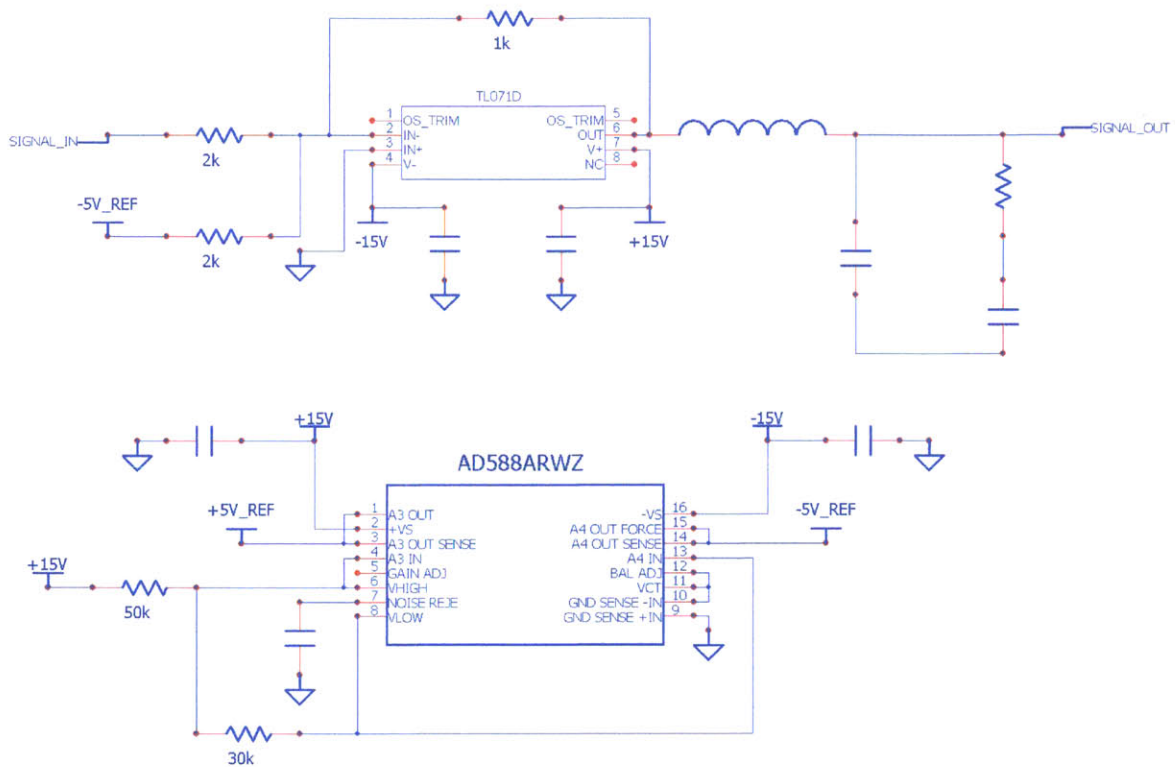


Figure 2-8: Top: one of six summing amplifier configurations used to shift signals up by +5V.

Bottom: Voltage reference circuit used to create steady $-5V$. Because minimal current is drawn by the summing amplifiers, all share the same $-5V$ reference.

Chapter 3

Final Layout

3.1 Physical Footprint

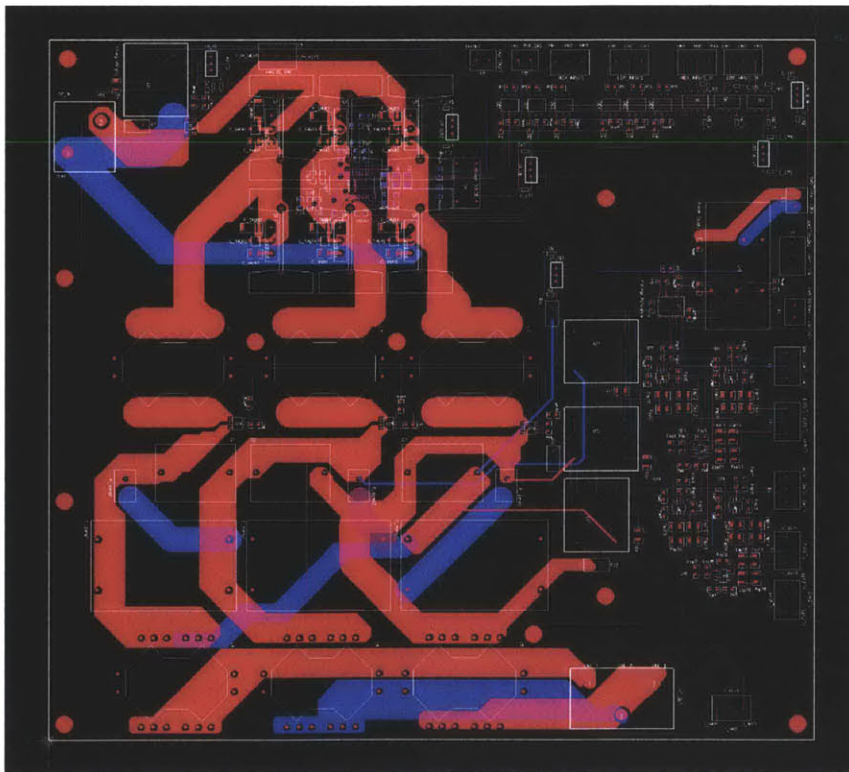


Figure 3-1: Overall view of circuit footprint. The ground planes are hidden in this view of the board.

The final circuit measures 12in wide by 10in tall and uses 4 total layers. One layer is reserved exclusively for ground planes to reduce noise, especially around the

MOSFETs and filters. There were several concerns when laying out the physical circuit. Most importantly, the traces handling the three-phase bridge and its output filters needed to be capable of handling up to 10A. It was conservatively calculated that these traces should have a width of at least 0.5in, although they are narrower at certain areas to route around the MOSFETs and current sensors. All control traces are 0.015in, while individual component power traces are 0.02in wide in order to distinguish them. All components which use heat sinks have had the heat sinks included in the design to accommodate for spacing.

To optimize switching speed and try to match any delays across all MOSFETs, the driver chip is mounted on the underside of the board, directly underneath the middle of the second phase of the totem bridge. This central location allows its gate drive outputs to be directed to the switches without the use of any vias or long, undesirable trace loops. The low-power control routes and circuit modules are placed on the top and right sides of the board, allowing for quick access to a wide assortment of I/O screw terminals while maintaining separation from the high-power area.

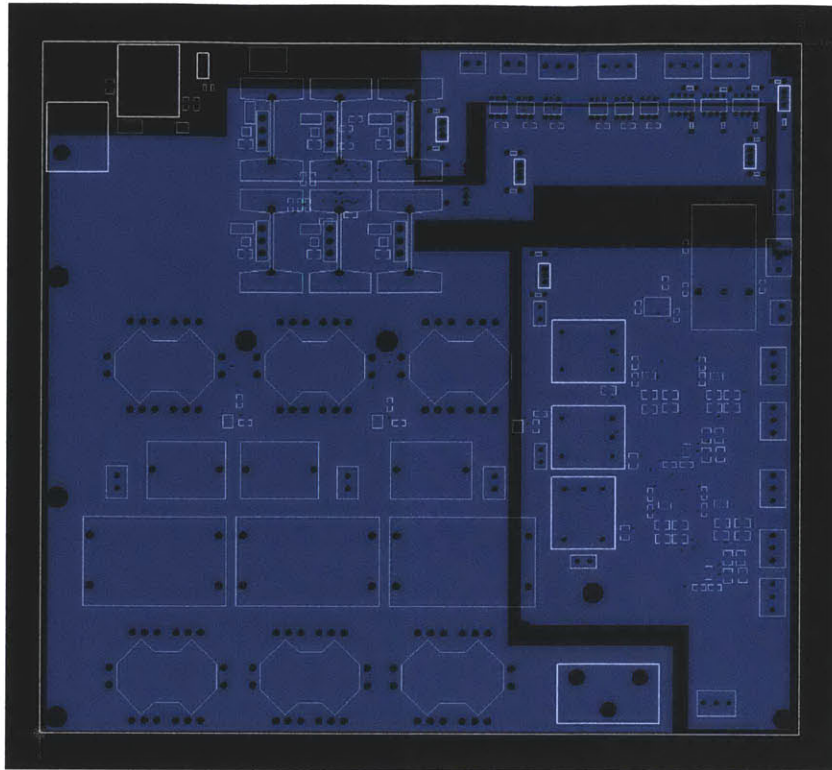


Figure 3-2: View of three separate ground planes in circuit. Component footprints are shown for reference.

The ground planes are shown in Figure 3-2. The largest plane exists under the entire high-power section as this will be most susceptible to noise. The top right plane lies below the digital inputs coming from the control hardware, and finally the rightmost plane is designed to ground all analog signals - the sensing and signal processing components. The digital and analog grounds should be connected through the use of the board's screw terminals that follow the top and right borders of the inverter. This single-point connection prevents any internal loops from being created in the trace, which would create unnecessary parasitic inductance.

3.2 Conclusion

The three-phase bridge is a common topology and further details of the inverter, such as certain component values, are dependent on the control scheme used to switch the MOSFETs. The inverter designed in this paper is intended to general purpose, and the finalized overall schematic is appropriate for any practical control scheme that may be used in the microgrid. The switching hardware and interface software discussed in Chapter 1 still remains in use and has proven to be both quick and intuitive to use, as originally intended. Though the microgrid itself is an ongoing project, the inverter itself has been developed to accommodate this in anticipation of future changes in the project.

Bibliography

- [1] A. H. Kasem Alaboudy, H. H. Zeineldin, and J. Kirtley. *Impact of DG Interface Control, Microgrid Control Strategy and Load Type on Microgrid Stability*, Masdar Institute of Science and Technology and MIT. 2011.
- [2] IEEE. *1547.2: IEEE Application Guide for IEEE Std 1547 IEEE Standard for Interconnecting Distributed Resources with Electric Power Systems*, chapter 8.1.5. 2009.
- [3] Jared Monnin. *Impact of Load Type on Microgrid Stability*. Master's thesis, MIT, 2010.
- [4] John G. Kassakian, Martin F. Schlecht, and George C. Verghese. *Principles of Power Electronics*, chapter 24.1. Addison-Wesley, 1991.
- [5] International Rectifier. *IR213 3-Phase Bridge Driver Data Sheet No. PD60166 revU*. 2008.
- [6] James Worden and Michael Zuercher-Martinson. "How Inverters Work". *SolarPro Magazine Issue 2.3*, Apr/May 2009.